Video Article

Super-resolution Imaging of the Bacterial Division Machinery

Jackson Buss[1], Carla Coltharp[1], Jie Xiao[1]

[1]Department of Biophysics and Biophysical Chemistry, The Johns Hopkins University School of Medicine

Correspondence to: Jie Xiao at jxiao@jhmi.edu

URL: https://www.jove.com/video/50048
DOI: doi:10.3791/50048

Keywords: Biophysics, Issue 71, Cellular Biology, Microbiology, Molecular Biology, Structural Biology, Chemistry, Physics, super-resolution imaging, PALM, FtsZ, mEos2, cell division, cytokinesis, divisome

Date Published: 1/21/2013

Citation: Buss, J., Coltharp, C., Xiao, J. Super-resolution Imaging of the Bacterial Division Machinery. *J. Vis. Exp.* (71), e50048, doi:10.3791/50048 (2013).

Abstract

Bacterial cell division requires the coordinated assembly of more than ten essential proteins at midcell[1,2]. Central to this process is the formation of a ring-like suprastructure (Z-ring) by the FtsZ protein at the division plan[3,4]. The Z-ring consists of multiple single-stranded FtsZ protofilaments, and understanding the arrangement of the protofilaments inside the Z-ring will provide insight into the mechanism of Z-ring assembly and its function as a force generator[5,6]. This information has remained elusive due to current limitations in conventional fluorescence microscopy and electron microscopy. Conventional fluorescence microscopy is unable to provide a high-resolution image of the Z-ring due to the diffraction limit of light (~200 nm). Electron cryotomographic imaging has detected scattered FtsZ protofilaments in small *C. crescentus* cells[7], but is difficult to apply to larger cells such as *E. coli* or *B. subtilis*. Here we describe the application of a super-resolution fluorescence microscopy method, Photoactivated Localization Microscopy (PALM), to quantitatively characterize the structural organization of the *E. coli* Z-ring[8].

PALM imaging offers both high spatial resolution (~35 nm) and specific labeling to enable unambiguous identification of target proteins. We labeled FtsZ with the photoactivatable fluorescent protein mEos2, which switches from green fluorescence (excitation = 488 nm) to red fluorescence (excitation = 561 nm) upon activation at 405 nm[9]. During a PALM experiment, single FtsZ-mEos2 molecules are stochastically activated and the corresponding centroid positions of the single molecules are determined with <20 nm precision. A super-resolution image of the Z-ring is then reconstructed by superimposing the centroid positions of all detected FtsZ-mEos2 molecules.

Using this method, we found that the Z-ring has a fixed width of ~100 nm and is composed of a loose bundle of FtsZ protofilaments that overlap with each other in three dimensions. These data provide a springboard for further investigations of the cell cycle dependent changes of the Z-ring[10] and can be applied to other proteins of interest.

Video Link

The video component of this article can be found at https://www.jove.com/video/50048/

Protocol

1. Sample Preparation

1. Inoculate LB media with a single colony of strain JB281 [BW25113 / pJB042 (P_{Lac}:FtsZ-mEos2)]. Grow overnight in a shaker at 37 °C.
2. Dilute the culture 1:1,000 into $M9^+$ minimal media [M9 Salts, 0.4% Glucose, 2 mM $MgSO_4$, 0.1 mM $CaCl_2$, MEM Amino Acids and Vitamins] and grow to mid-log phase (OD_{600}= 0.2-0.3) in the presence of chloramphenicol (150 µg/ml) at room temperature (RT).
3. Induce culture with 20 µM IPTG for 2 hr (see Note #1).
4. Pellet culture in microcentrifuge (8,000 rpm, 1 min) and resuspend in an equal volume of $M9^+$; repeat. After the second resuspension, continue growth at RT for 2 hr.
5. Fix induced culture with 4% paraformaldehyde in PBS (pH=7.4) at RT for 40 min. Pellet culture and resuspend in an equal volume of PBS; repeat. If imaging live cells, skip fixation, pellet culture, and resuspend with equal volume of $M9^-$ [M9 Salts, 0.4% Glucose, 2 mM $MgSO_4$, 0.1 mM $CaCl_2$, MEM Amino Acids]; repeat.
6. Dilute gold beads 1:10 with resuspended culture. Apply sample to prepared imaging chamber (see step 2.4).

[1] Note: The above induction protocol (steps 1.1-1.3) has been optimized for the expression system of strain JB281. Detailed induction conditions may vary for other expression systems or proteins of interest.

2. Assembly of the Imaging Chamber

1. Make a 3% (w/v) agarose solution in $M9^-$. Melt agarose at 70 °C in a bench-top heat block for 40min. Store melted agarose at 50 °C for up to 5 hr.

2. Place a clean microaqueduct slide in the upper half of the imaging chamber with the electrodes facing down. Align the lower gasket on the microaqueduct slide so as to cover the perfusion channels.
3. Apply ~50 µl of the melted agarose to the center of the glass slide. Immediately top the agarose gel droplet with a clean, dry coverslip. Allow the gel to solidify at RT for 30 min.
    1. To clean coverslips: arrange coverslips in a ceramic holder and sonicate for 20 min in rotating baths of acetone, ethanol and 1M KOH in glass jars. Repeat cycle three times, for a total of 9 sonications, followed by a single sonication in dH_2O. Store the cleaned coverslips in fresh dH_2O. Prior to use, blow dry coverslips with filtered air.
4. Carefully remove coverslip, leaving gel pad on the microaqueduct slide. Immediately add 1 µl of cell culture sample (see step 1.6) to the top of the gel pad. Wait for ~2 min, allowing solution to be absorbed by the gel pad. Top gel pad with a new clean, dry coverslip. Assemble the whole imaging chamber according to manufacturer's instructions.

3. Image Acquisition

1. Turn on the microscope, camera and lasers. Open MetaMorph software (Molecular Devices).
2. Place appropriate excitation/emission filters in the imaging path (**Figure 1**).
3. Set laser powers and acquisition settings accordingly.
    1. 488-nm laser = 15 mW (see Note #2)
    2. 561-nm laser = 75 mW
    3. 405-nm laser = 2 mW ± neutral density filter (see Note #3)
4. Lock imaging chamber into the stage via the complementary stage adaptor.
5. Designate an appropriate imaging region (100x100 pixel) that is homogenously illuminated by all three lasers.
6. Identify a sample area that contains both cells and fiducial markers (gold beads) in close proximity but not overlapping.
7. Focus on the surface of cells closest to the coverslip. Acquire one brightfield image with 50 ms integration time and move the focus 0.5 µm into the sample (**Figure 3Ai**).
8. Acquire ensemble green fluorescence image with excitation from the 488-nm laser using a 50 ms integration time (**Figure 3Aii**).
9. Acquire streaming video in red channel with continuous illumination from 405-nm and 561-nm lasers. For fixed cells, a 50 ms frame rate is used for a total of 20,000 frames (~17 min total) with the 405-nm laser power ramped by ~10% every 1,000 frames (see Note #4). For live cells, a 10 ms frame rate is used for a total of 3,000 frames (~30 s total) at a constant 405-nm laser power.
10. Move the focus back to the lower surface of the cells and acquire another brightfield image as in step 3.7.

[2] Note: The integrated intensity of the green fluorescence of a cell is directly proportional to the total number of FtsZ-mEos2 molecules expressed in the cell. The 488-nm excitation power and ensemble fluorescence acquisition settings should be kept constant for all cells so that the relative FtsZ-mEos2 expression levels in different cells can be compared.

[3] Note: Fixed cells are imaged with the Neutral Density (ND) filter (**Figure 1**, Optical Component #5) in place in order to achieve a slow activation rate so that each individual molecule can be accurately identified. The ND filter is removed when imaging live cells to increase the activation rate, while maintaining a low probability of two molecules being activated simultaneously in a diffraction-limited area. The faster rate applied to live-cell imaging is needed to decrease the total acquisition time, thereby "freezing" the Z-ring in time and limiting the effect of photodamage to the cell.

[4] Note: The numbers of frames acquired were optimized for our system and are dependent on the particular cellular structure, labeling density, activation rate and whether exhausting the entire pool of fluorophores is important for analysis. In live cells, it is important to obtain a sufficient number of localizations in as short a period of time as possible to avoid the blurring of the image due to movement of the cellular structure.

4. PALM Image Construction

1. Determine centroid position of each detected spot.
    1. Load the image stack into Matlab (MathWorks, Inc).
    2. Crop the image stack to a region around one cell that excludes all fiducial beads.
    3. Select an intensity threshold for spot detection that is above the background level, but below the average spot intensity. We account for the variation in background level throughout an experiment by calculating the running average of maximum intensity using a 150 frame window. The intensity threshold for each frame is then interpolated from the running average values.
    4. Subtract the respective threshold from each frame. Prospective spots are identified as three adjacent pixels with intensities above threshold.
    5. Fit the fluorescence intensity of each prospective spot to a two-dimensional Gaussian function [Equation #1] using a nonlinear least squares algorithm (**Figure 2**). The localization precision of each spot is calculated using the total number of detected photons [Equation #2]. Any poorly-fit spot with a localization precision greater than 20 nm (fixed cells) or 45 nm (live cells) is discarded (see Note #5). Any spot with an intensity greater than two-fold of the mean intensity, possibly due to overlapping emitters, is also discarded.
    6. For fixed cells, remove repeated observations of the same molecule by disregarding any spot whose centroid position is within 45 nm of any other spot that preceded it by 6 frames or less. For live cells, all spots are retained.
2. Calibrate sample drift using fiducial marker movement.
    1. Crop out a 10x10 pixel region around a fiducial marker.
    2. Subtract the respective threshold determined in 4.1.3 from each frame.
    3. Fit the intensity profile in each frame via least-square fitting algorithm assuming a two-dimensional Gaussian shape.
    4. Calculate displacement between centroid positions relative to frame 1.

3. Correct the centroid position of each unique molecule identified in 4.1 with the appropriate sample drift calculated in 4.2. Compare the brightfield images acquired in 3.7 and 3.10. If cells are observed to move relative to the fiducial markers, the data is thrown out.
4. Superimpose all corrected centroid positions on a single image composed of 15x15 nm pixels. Plot each unique molecule as a unit-area, two-dimensional Gaussian profile centered at the centroid position with a standard deviation equal to the localization precision [Equation #2]. This results in a probability density map, where a pixel's intensity is proportional to the likelihood of finding a molecule in that pixel (**Figure 3Aiv**).
5. Comparing PALM images to ensemble images.
    1. Replot the centroid positions as in 4.4, but on a plane with 150x150 nm pixels and a standard deviation equal to 250 nm. This generates a PALM image that mimics a diffraction-limited image, which can be used to compare to the diffraction-limited, ensemble image acquired in 3.8 (**Figure 3Aiii**).
    2. To confirm that the detected molecules are representative of the whole population, compare the reconstructed ensemble image (**Figure 3Aiii**, step 4.5.1) with the experimental ensemble fluorescence image (**Figure 3Aii**, step 3.8) to confirm that both images show structures of similar shape, orientation and relative intensity.

[5] Note: The minimum required localization precision was determined empirically for each imaging method by plotting the precisions of all molecules for a given sample and selecting an appropriate cutoff.

5. PALM Image Analysis

1. Measuring Z-Ring Width and Diameter.
    1. Rotate the PALM image so as to vertically orient the long axis of the cell (**Figure 4A**).
    2. Crop out the cellular region containing the Z-ring.
    3. Calculate the cumulative intensity by projecting an intensity profile along the cell's long axis.
    4. Fit the intensity profile to a Gaussian distribution. The ring width is defined as the full width half maximum (FWHM) of the fitted Gaussian distribution (**Figure 4B**).
    5. Project the cumulative intensity profile of 5.1.2 along the cell's short axis. The ring diameter is defined as the full length of the intensity profile (**Figure 4C**).

2. Plotting FtsZ Density (see Note #6).
    1. Replot the centroid positions as in (4.4), but without the Gaussian profile such that each unique molecule is given a value of 1 and assigned to a single pixel corresponding to its centroid position. In this way, the intensity of each pixel represents the total number of molecules detected in that pixel. The Density PALM image can also be visualized as a contour plot (**Figure 5E**).

3. Determining Spatial Resolution.
    1. Theoretically-achievable spatial resolution: create a representative PSF for the entire sample using the average determined localization precision of all detected molecules and calculate the FWHM (Equation #3).
    2. Experimentally-achieved spatial resolution: calculate the average displacement between repeat observations of the same molecule.

[6] Note: We used total internal reflection PALM (TIR-PALM, **Figure 1** and **5**) to restrict the activation and excitation to a thin layer (~200 nm) above the cell/glass interface. so that only FtsZ molecules associated with the membrane closest to the coverslip will be detected.

Representative Results

Illustrated in **Figure 3Aiv** is a two-dimensional, super-resolution rendering of the Z-ring generated from the PALM imaging method described above. Below, we summarize qualitative and quantitative information that can be obtained from them.

Qualitatively, we observed that the Z-ring is an irregular structure that adopts multiple configurations (single band or helical arc) that are not distinguishable in conventional fluorescence images (compare **Figure 3A-Dii** and **iv)**. Observations such as these can be used to determine the percent of the cell population that displays a particular structural configuration.

We can also quantitatively measure the dimensions of the Z-ring. Our approach for determining the ring width and diameter are described in step 5.1 and illustrated in **Figure 4**. From **Figure 4B**, the ring width was determined to be 113 nm (FWHM). This value is wider than the expected width of a single FtsZ protofilament (5-10 nm based on *in vitro* EM[11]). In **Figure 4C**, the ring diameter is measured as 1,050 nm. This diameter can be used to quantitatively describe the degree of constriction during cell division.

Another quantitative approach is to calculate the molecule density by counting the number of molecules localized within a defined region. The density measurement provides information about how tightly molecules are packed in the structure. Molecule density can be described in both relative and absolute terms. Relative density (*e.g.* fraction of molecules in the Z-ring vs. the whole cell) provides information about the distribution of molecules into different cellular regions. Absolute density measurement is complicated by the fact that the PALM image (**Figure 3Aiv**) is actually a 2D projection of a 3D object. To circumvent this complication, we employ TIR-PALM, which restricts the detection plane to a single side of the Z-ring. The resulting data is illustrated in **Figure 5E**. Since the plotted molecules represent a subset of the total FtsZ population, the density determined is a lower limit of the actual density. The maximal density observed in the TIR images of the Z-ring suggest that some sections contain overlapping protofilaments [10].

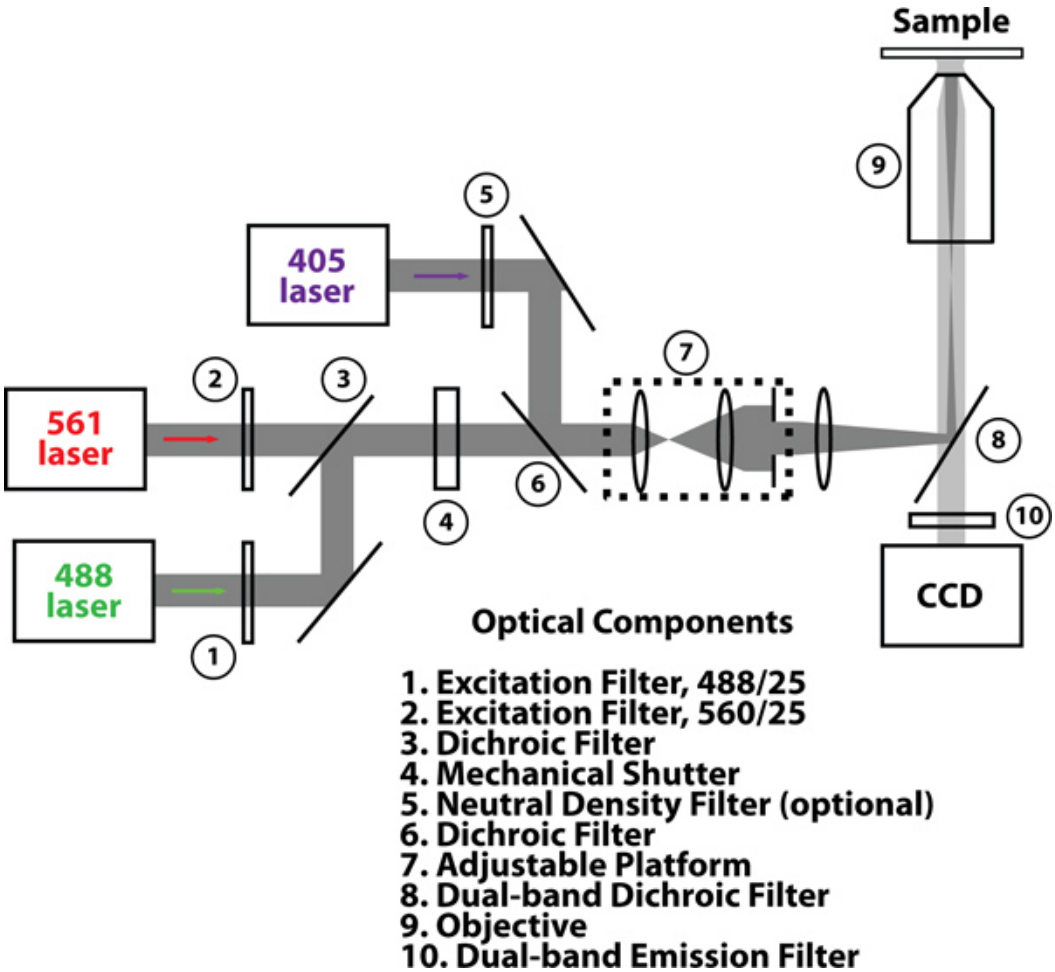

Figure 1. A simplified schematic of our microscope setup. All three lasers are controlled by a custom imaging program developed in MetaMorph that enables precise control over the appropriate excitation wavelength. The dark gray line indicates the excitation light path, while the light gray line indicates the emission path. For total internal reflection (TIR) microscopy, the adjustable platform is translated perpendicular to the light path so as to change the incident angle.

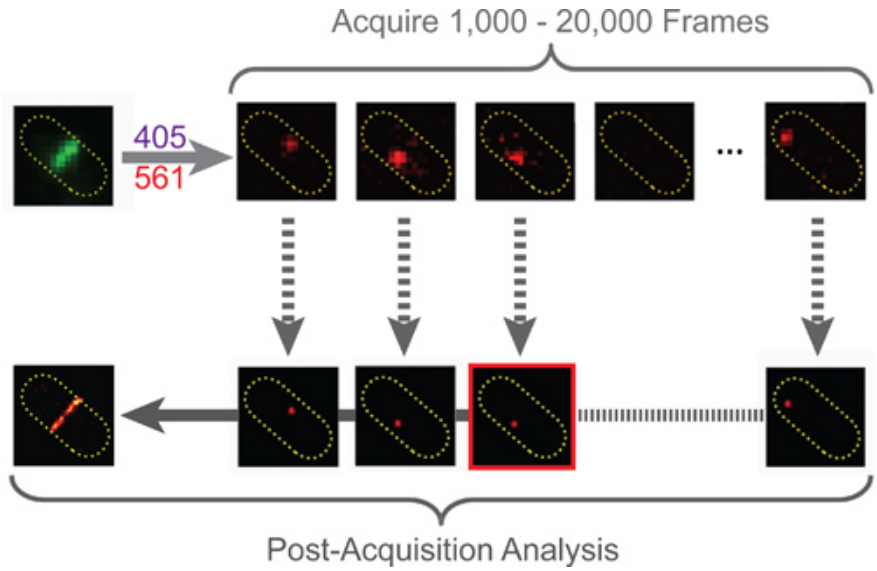

Figure 2. A summary of the PALM method. Initially, all FtsZ-mEos2 molecules are in the green-fluorescence state. Upon exposure to continuous illumination by the 405 and 561 lasers, single molecules are stochastically converted to the red fluorescence state. The rate of this process is determined by the power of the 405 laser, while the photobleaching rate is determined by the power of both the 405 and the 561 laser. Ideally, the rate of activation and photobleaching are balanced in such a way that only one molecule is detected per frame. Once a sufficient number of frames are acquired, the images are processed in Matlab by fitting each identified spot as described in step 4.1. Each unique molecule is then plotted (step 4.4) on a single plane, thus generating a PALM image, shown here in pseudo-red color. The frame outlined in red was determined to contain a repeat spot from the same molecule as the preceding frame and was therefore not included during the construction of the PALM image.

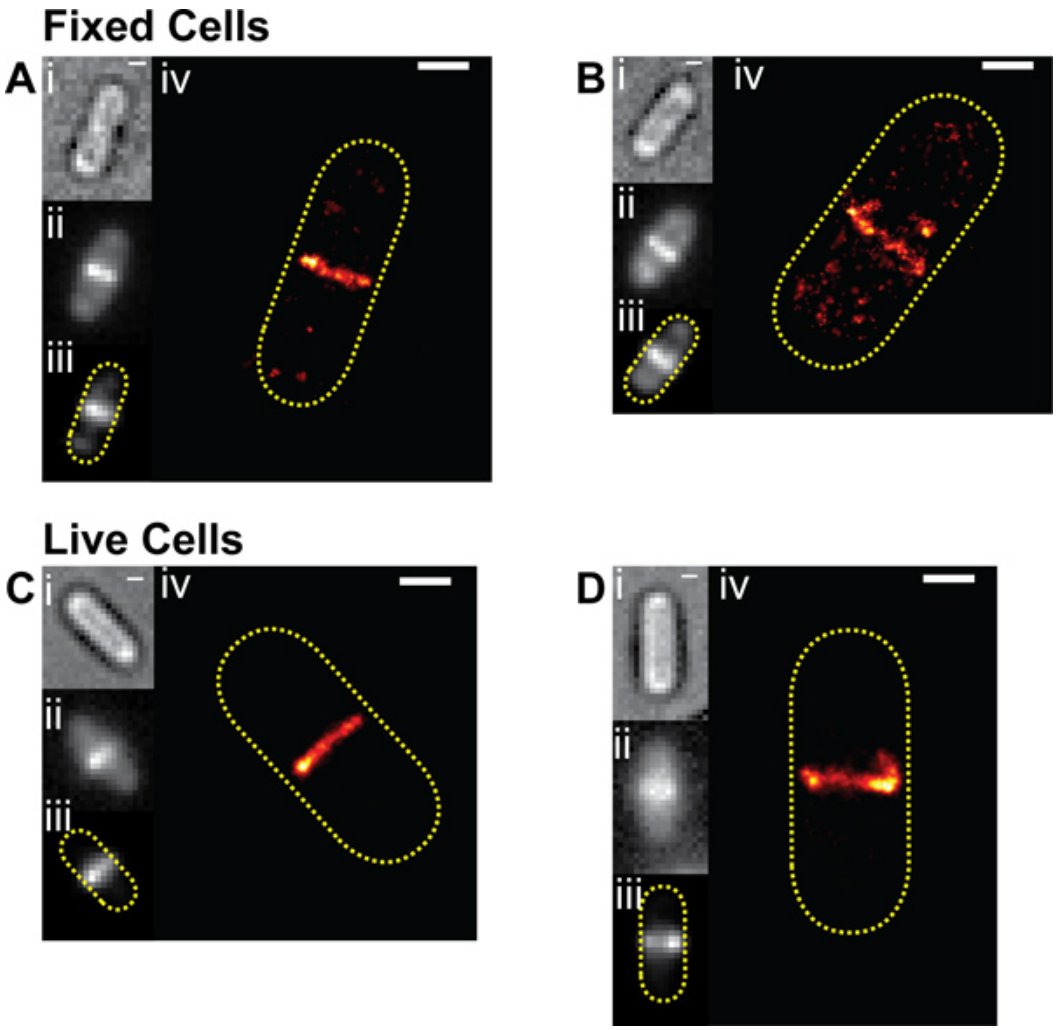

Figure 3. Representative images of fixed (A and B) and live (C and D) cells expressing FtsZ-mEos2. For all cells, the outline and general shape can be visualized in the brightfield image (**i**). Ensemble fluorescence images (**ii**) are acquired with excitation from the 488 laser (step 3.8) and represent the distribution of the entire pool of FtsZ-mEos2. The ensemble image reconstructed from the PALM data (**iii**, step 5.4) provides a qualitative check for the method's faithful representation of the true ensemble structure. The generated PALM image (**iv**) is the summation of all unique FtsZ-mEos2 localizations and represents a probability density map for FtsZ-mEos2. The cell outline is represented by the yellow dotted line in images **iii** and **iv**. Cells A and C show FtsZ in a single band conformation, while cells B and D illustrate FtsZ adopting a helical arc conformation, which is undetectable in the diffraction-limited ensemble image (**iii**). Scale bars, 500 nm.

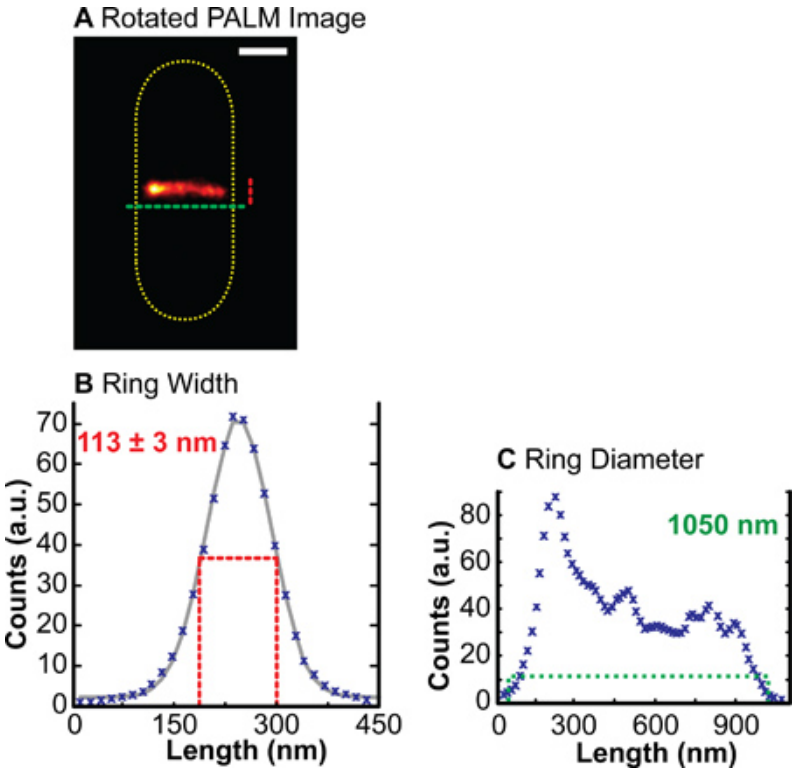

Figure 4. A. A PALM image showing schematic representations of Z-ring width (red) and Z-ring diameter (green). **B.** Ring width is calculated by fitting the projected intensity profile (blue X's) along the long axis of the cell with a Gaussian function (gray line) and then determining the FWHM (red dotted line). Here, the ring width was determined to be 113 nm. **C.** Ring diameter is determined by first projecting the intensity profile along the short axis of the cell and then calculating the full length (green dotted line) of the intensity profile above zero. The diameter of the Z-ring was determined to be 1,050 nm.

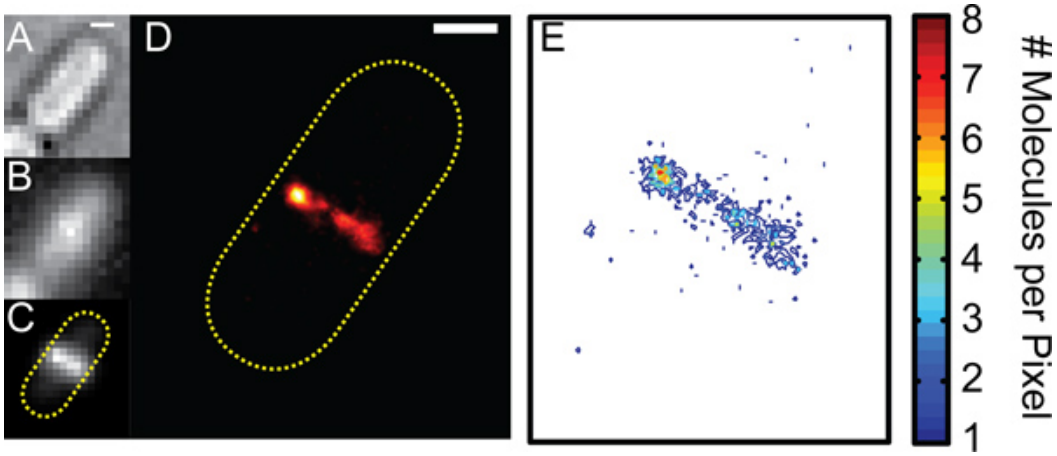

Figure 5. TIR-PALM allows for the accurate counting of molecules. As in **Figure 3**, the brightfield image (**A**), ensemble fluorescence image (**B**), reconstructed ensemble fluorescence image (**C**) and PALM image (**D**) are illustrated for a given cell expressing FtsZ-mEos2. The same data used to construct **D** is replotted as a contour plot of molecule density (molecules per pixel) in **E**. From this density analysis, FtsZ-mEos2 was determined to be maximally present at 8 molecules per pixel. Because a single layer of FtsZ protofilaments would result in a maximum density of 5 molecules per pixel[10], this analysis suggests that the Z-ring is composed of multiple layers of FtsZ protofilaments.

Discussion

PALM images contain information about molecule counts and positions within a cell, allowing detailed analysis of the distribution and arrangement of target protein molecules that is difficult to achieve by other means. Below we outline precautions that should be taken to extract accurate quantitative information while maintaining the biological relevance of PALM images. We also explore the information that can be best obtained using live vs. fixed cells. Finally, we suggest avenues for obtaining additional super-resolution information about the cell division machinery.

The method described above was optimized to produce accurate PALM images in the following ways. First, we characterized and optimized the functionality of the fusion protein to ensure that it serves as a reliable marker of Z-ring structure[10]. Second, we fine-tuned the expression of

the fusion protein since both over- and under-expression results in aberrant structure formation [10,12,13]. Third, we chose thresholds for unique molecule determination (step 4.1.5) based on fluorophore photoblinking properties[14]. Photoblinking complicates the determination of unique molecules and if disregarded, leads to overcounting of single molecules. Although overcounting does not affect dimension measurements, it does amplify absolute density measurements and may create the appearance of false clusters. All of these factors should be carefully considered when applying this method to other proteins of interest.

The selection of live or fixed cells for imaging depends on the desired information and throughput. Live-cell imaging is fast (30 s), but only reports on localizable (*i.e.* slow-moving) molecules. This usually means that only membrane-associated molecules are observed in live cells, while fixed cells provide information on all labeled molecules. Live-cell imaging provides high-resolution structural dimensions and morphology, but cannot provide accurate molecule density measurements due to the movement of individual molecules. Fixed cell images can provide all of this information, but require low UV activation level so that unique molecules can be identified. This leads to extended imaging times (> 15 min). In addition, fixation may cause structural aberrations. All of these factors should be balanced when choosing which sample type to use.

The PALM method we have described provides super-resolution details of the Z-ring structure that can be compared across different strains, cell-cycle states, and growth conditions. Implementation of recent technological advances may provide added insight in the cytokinetic mechanism of the Z-ring. For instance, introducing astigmatism into the detection pathway is the simplest way to add three-dimensional capability (~100 nm z-resolution) to the optical setup illustrated in **Figure 1**[15]. Also, simultaneously imaging of two or more proteins at the same time has become a realistic option with the rapid emergence of spectrally-distinct photoactivatable fluorescent proteins. Finally, the development of a fluorescent protein that photoactivates in a UV-independent manner would allow long-term monitoring of a single cell without generating the DNA damage induced by 405 nm illumination.

Disclosures

No conflicts of interest declared.

Acknowledgements

Grant: 5RO1GM086447-02.

References

1. Buddelmeijer, N. & Beckwith, J. Assembly of cell division proteins at the *E. coli* cell center. *Curr. Opin. Microbiol.* **5**, 553-557 (2002).
2. de Boer, P., Crossley, R., & Rothfield, L. The essential bacterial cell-division protein FtsZ is a GTPase. *Nature.* **359**, 254-256 (1992).
3. Lutkenhaus, J.F., Wolf-Watz, H., & Donachie, W.D. Organization of genes in the ftsA-envA region of the *Escherichia coli* genetic map and identification of a new fts locus (ftsZ). *J. Bacteriol.* **142**, 615-620 (1980).
4. Bi, E.F. & Lutkenhaus, J. FtsZ ring structure associated with division in *Escherichia coli. Nature.* **354**, 161-164 (1991).
5. Erickson, H.P., Taylor, D.W., Taylor, K.A., & Bramhill, D. Bacterial cell division protein FtsZ assembles into protofilament sheets and minirings, structural homologs of tubulin polymers. *Proc. Natl. Acad. Sci. U.S.A.* **93**, 519-523 (1996).
6. Osawa, M., Anderson, D.E., & Erickson, H.P. Reconstitution of contractile FtsZ rings in liposomes. *Science.* **320**, 792-794 (2008).
7. Li, Z., Trimble, M.J., Brun, Y.V., & Jensen, G.J. The structure of FtsZ filaments *in vivo* suggests a force-generating role in cell division. *Embo J.* **26**, 4694-4708 (2007).
8. Betzig, E., *et al.* Imaging intracellular fluorescent proteins at nanometer resolution. *Science.* **313**, 1642-1645 (2006).
9. McKinney, S.A., Murphy, C.S., Hazelwood, K.L., Davidson, M.W., & Looger, L.L. A bright and photostable photoconvertible fluorescent protein. *Nat. Methods.* **6**, 131-133 (2009).
10. Fu, G., *et al. In-vivo* FtsZ-ring structure revealed by Photoactivated Localization Microisocpy (PALM). *Plos One.*, (2010).
11. Huecas, S., *et al.* Energetics and geometry of FtsZ polymers: nucleated self-assembly of single protofilaments. *Biophys. J.*, (2007).
12. Ma, X., Ehrhardt, D.W. & Margolin, W. Colocalization of cell division proteins FtsZ and FtsA to cytoskeletal structures in living *Escherichia coli* cells by using green fluorescent protein. *Proc. Natl. Acad. Sci. U.S.A.* **93**, 12998-13003 (1996).
13. Dai, K. & Lutkenhaus, J. The proper ratio of FtsZ to FtsA is required for cell division to occur in Escherichia coli. *J. Bacteriol.* **174**, 6145-6151 (1992).
14. Annibale, P., Vanni, S., Scarselli, M., Rothlisberger, U., & Radenovic, A. Identification of clustering artifacts in photoactivated localization microscopy. *Nat. Meth.* **8**, 527-528 (2011).
15. Huang, B., Wang, W., Bates, M., & Zhuang, X. Three-dimensional super-resolution imaging by stochastic optical reconstruction microscopy. *Science.* **319**, 810-813 (2008).

